Combustion Condition Recognition of Coal-Fired Kiln Based on Chaotic Characteristics Analysis of Flame Video

Yu Jiang, Hua Chen, Xiaogang Zhang, *Member, IEEE*, Yicong Zhou, *Senior Member, IEEE*, and Lianhong Wang

***Abstract*—Keeping combustion stable and detecting unstable states in time is crucial for coal-fired furnaces such as rotary kilns, boilers, and oxygen furnaces. Because of the interference and complex conditions in the industrial field, recognition of combustion conditions by vision analysis is difficult. In this article, we propose a robust nonlinear dynamic system analysis-based approach for combustion condition recognition by extracting chaotic characteristics from a flame video. We first discover chaotic characteristics in the intensity sequence extracted from a flame video of coal-fired kilns, and then we further find that the underlying chaos rules differ between combustion conditions. Based on this finding, we design a set of trajectory evolution features and morphology distribution features of chaotic attractors for combustion condition recognition. After reconstructing the chaotic attractors from the intensity sequence of a flame video by phase space reconstruction, the quantified features are extracted from the recurrence plot and morphology distribution and put into a decision tree to recognize the combustion condition. The experimental results on real-world data show that the proposed method can recognize the combustion condition in coal-fired kilns effectively and promptly. Compared with other methods, the recognition accuracy is improved more than 5%.**

***Index Terms*—Chaotic characteristics, combustion condition, flame video, morphology distribution features (MDFs), trajectory evolution features (TEFs).**

Manuscript received April 13, 2021; revised August 9, 2021 and September 17, 2021; accepted October 1, 2021. Date of publication October 6, 2021; date of current version February 18, 2022. This work was supported in part by the National Key Research and Development Program of China under Grant 2018YFB1305900, in part by the National Natural Science Foundation of China under Grant 62171184 and Grant 62106072, and in part by the Science and Technology Innovation Program of Hunan Province under Grant 2020GK2020. Paper no. TII-21-1657. *(Corresponding author: Xiaogang Zhang.)*

Yu Jiang, Xiaogang Zhang, and Lianhong Wang are with the College of Electrical and Information Engineering, Hunan University, Changsha 410082, China (e-mail: jy199548@hnu.edu.cn; zhangxg@hnu.edu.cn; wanglh@hnu.edu.cn).

Hua Chen is with the College of Computer Science and Electronic Engineering, Hunan University, Changsha 410082, China (e-mail: chua@hnu.edu.cn).

Yicong Zhou is with the Department of Computer and Information Science, University of Macau, Macau 999078, China (e-mail: yicongzhou@um.edu.mo).

Color versions of one or more figures in this article are available at https://doi.org/10.1109/TII.2021.3118135.

Digital Object Identifier 10.1109/TII.2021.3118135

I. Introduction

ANALYSIS of the combustion state is involved in many combustion-related industrial processes, such as power generation and cement and steel production. Maintaining stable combustion is related to safe production, economy, and environmental protection. Unstable combustion conditions can lead to high pollutant emissions, low efficiency, and uneven heat distribution. Therefore, detecting unstable combustion conditions in a timely and accurate manner is a key technical bottleneck that urgently needs to be resolved.

Combustion condition analysis can be divided into two categories: mechanism modeling and data-driven modeling. A mathematical model is established to detect abnormal combustion conditions according to the basic principles of reaction chemistry, solid-phase kinetics, and heat transfer mechanisms. Usually, the heat flow [1] and the radiation of the temperature field [2] in the furnace are studied by controlling the air-fuel ratio [3]. Compared with laboratory conditions, the industrial environment is harsh and involves many industrial factors, and theoretical mechanism models are difficult to employ in practice. In this case, data-driven modeling provides an effective alternative.

Data-driven modeling methods recognize combustion conditions by mining the characteristics of the flame image or thermal data obtained by a distributed control system. Vision-based modeling uses image and video information for prediction or pattern recognition. The flame image contains a wealth of production information, such as product quality, changes in working conditions, and equipment status. Therefore, flame image-based modeling methods have been widely applied to detect combustion ON/OFF [4], clinker quality [5], sintering [6], [7], and stability conditions [8], [9] in furnaces, such as power plant boilers [10], biomass boilers [11], gas turbines [12], etc.

In terms of combustion stability analysis, representative methods include, first, extracting features only from flame images; second, combining flame features with features extracted from thermoacoustic signals, luminescence imaging of OH/CO chemical emissions, or radiation signals; and finally, combining the flame image feature extraction process with the recognition process to form an end-to-end combustion stability analysis

Fig. 1. Flame images taken in the coal-fired burner.

method via a deep neural network (DNN) or convolutional neural network.

For the first category, typical image features such as color [13], edge roughness [14], oscillation frequency [8], spatial variation, and movement [15] are extracted for diagnosis. Najarnikoo *et al.* [13] studied the reliable relationship between digital image color and flame characteristics in the visible light domain and found the best combustion running conditions, which can be defined as the intersection of the two intensity components of red and blue. Matthes e*t al.* [15] proposed a geometric interpretation to obtain the best threshold of the flame area. Sun *et al.* [16] proposed the universal index and oscillation frequency. These two indicators were used to evaluate the flame color, geometry, and brightness and then detect the flame stability of heavy oil fuel burners. These typical image feature extraction methods are mostly based on image extraction. After segmenting the flame part, the feature is extracted. However, if the image is unclear, incorrect image segmentation will eventually lead to the failure of combustion condition recognition. Therefore, some scholars analyze the image together with other thermal signals. Yilmaz *et al.* [17] observed flame burning under the external sound pressure generated by two speakers and comprehensively considered the dynamic pressure and static pressure collected by the pressure gauge to evaluate the flame stability. To avoid incorrect manual features and automatically learn representative features, some scholars proposed end-to-end combustion stability analysis strategies through deep learning. Han *et al.* [18] proposed a new method for monitoring combustion stability based on a stacked sparse autoencoder DNN. The proposed autoencoder was used to extract flame. Wang *et al.* [19] proposed a novel method based on a DNN to identify the combustion condition of a furnace and measure the heat release rate at the same time. They also implemented smoothing and adjustment techniques to make a trade-off between stability and sensitivity.

Most of the abovementioned research aims to detect the combustion condition (stable state /unstable state) in the test rig in the laboratory. In the context of coal-burning industries such as rotary kilns, the effects of these methods are not satisfactory. There are the following two main reasons.

1) Images taken by industrial cameras on-site are blurry because of the presence of dust particles and smoke, as shown in Fig. 1. It is difficult to extract the features from images accurately, which leads to the inaccuracy of relying on images for combustion condition recognition.
2) Combustion is a dynamic procedure, and the stable and unstable conditions refer to the operation of the system over time. Fig. 2 illustrates two typical intensity sequences formed by the average grey value of the flame image under two combustion conditions: unstable (Data1) and stable (Data2). We can see that the combustion condition is difficult to judge from a single image, but it can be distinguished if considering the fluctuation of intensity over time.

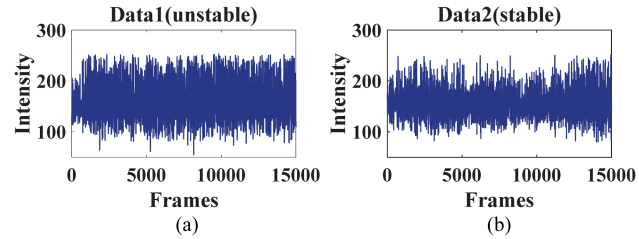

Fig. 2. Intensity sequences. (a) Data1 (unstable). (b) Data2 (stable).

Some studies have been carried out under industrial combustion conditions based on the flame image sequence and have achieved good effects [15], [16], [20]. Combustion is severely influenced by a variety of raw material ingredients and environmental factors, resulting in nonlinear, time-delayed, and variable characteristics of a flame video. Studying the nonlinear dynamic characteristics of time-series data in industrial combustion systems and analyzing the dynamic evolution law under different combustion conditions are vital for combustion condition analysis.

Chaos and chaotic characteristics have been proven to exist in much industrial data [21], [22]. Our previous studies have proven that there are chaos [23] and chaotic fractal characteristics [24] in the thermal signals and noise data in a rotary kiln. In this article, we further focus on the intensity sequence of a flame video and study its nonlinear dynamic characteristics. After that, we propose a combustion condition recognition approach based on the chaotic characteristics of a flame video.

The procedure of our robust combustion condition analysis method is as follows. First, we extract the intensity sequence from a flame video. Then, the intensity sequence is projected into a high-dimensional phase space to form a chaotic attractor by phase space reconstruction (PSR) [25] algorithm. The mutual information (MI) [26] and false nearest neighbor (FNN) [27] method is employed to estimate delay time τ and embedding dimension m. To study the trajectory evolution of chaotic attractors, recurrence plot (RP) [28] is employed, and five trajectory evolution features (TEFs) are calculated. To quantify the morphological characteristics of the attractor, we construct high-dimensional MD features (MDFs). Finally, the extracted features are input into the decision tree to obtain the recognition result.

The main contributions of this article are summarized as follows.

1) We first discovered that chaotic characteristics exist in the intensity sequence of an industrial flame video and substantially differ between combustion conditions.
2) We designed a set of TEFs and MDFs to quantify the trajectory and morphological characteristics of chaotic attractors in high-dimensional phase space.
3) We proposed a robust approach based on chaos dynamic system analysis for industrial flame video combustion

condition recognition, and it achieves a high recognition accuracy rate.

The rest of this article is organized as follows. In Section II, the characteristics of the chaotic attractor and flame video are analyzed. We discover that as long as the operation rules of the system remain unchanged, the morphological and evolutionary features of the system attractor are invariant. Furthermore, we also verify the chaotic characteristics of the intensity sequence of the flame video. In Section III, we design a set of TEFs and MDFs for quantifying the chaotic characteristics of a flame video, and we find that there are substantial differences between flame videos of stable and unstable conditions. Section IV presents the experimental results on real data for combustion condition recognition and robustness tests. Additionally, the state-of-the-art combustion condition analysis methods are compared in this section. Finally, Section V concludes this article.

II. Chaotic Characteristics of Flame Video

A. Chaos System

A dynamic system refers to a system whose state changes over time. The purpose of system evolution is embodied as a certain set of points in phase space, and the ultimate state of the evolution process is the attractor. The chaos phenomenon is a deterministic and stochastic process that appears in a nonlinear dynamic system. This process is neither periodic nor convergent and has a sensitive dependence on the initial value. The attractor of a chaotic system is called a chaotic attractor. The evolution trajectory and form of the chaotic attractor can reflect the internal operation rules of the dynamic system.

B. Characteristics of the Chaotic Attractor

Although the chaotic attractor is very sensitive to the initial value, the morphological and evolution characteristics of chaotic attractors are basically invariant if the operation rules are unchanged. Taking Lorenz [29], Rössler [30], and Chen's [31] attractors as examples, we choose the $x(t)$ variables in Lorenz, Rössler, and Chen's systems to reconstruct the phase space. And we give the formulas for these three systems in order as shown in the following:

$$\begin{cases} \frac{dx(t)}{dt} = a(y(t) - x(t)) \\ \frac{dy(t)}{dt} = bx(t) - y(t) - x(t)z(t) \\ \frac{dz(t)}{dt} = x(t)y(t) - c \end{cases} \tag{1}$$

$$\begin{cases} \frac{dx(t)}{dt} = -y(t) - x(t) \\ \frac{dy(t)}{dt} = x(t) + a * y(t) \\ \frac{dz(t)}{dt} = b + z(t)(x(t) - c) \end{cases} \tag{2}$$

$$\begin{cases} \frac{dx(t)}{dt} = a * (y(t) - x(t)) \\ \frac{dy(t)}{dt} = (c - a) * x(t) - x(t) * z(t) + c * y(t) \\ \frac{dz(t)}{dt} = x(t) * y(t) - b * z(t) \end{cases} \tag{3}$$

where $a = 36$, $b = 8/3$, $c = 28$ in (1), $a = 0.1$, $b = 0.2$, $c = 5.7$ in (2), and $a = 36$, $b = 8/3$, $c = 28$, in (3).

The PSR algorithm is usually the first step to investigate the chaotic characteristics of nonlinear signals. The basic essence of PSR algorithm is a projection of 1-D time-series data into a multidimensional space, which is topologically equivalent to the original one. Therefore, the reconstructed phase space can restore the dynamics of the original signal. The time delay method proposed by Takens embeds a one-dimension time-series x_i into a multidimensional time-series X_i [25], shown as follows:

$$\mathrm{X}_i = (x_i, x_{i+\tau}, x_{i+2\tau}, \ldots, x_{i+(m-1)\tau}) \tag{4}$$

where τ is the delay time, m is the minimum embedding dimension, and each X_i is a point in the m-dimensional phase space, representing the state of the system at time i.

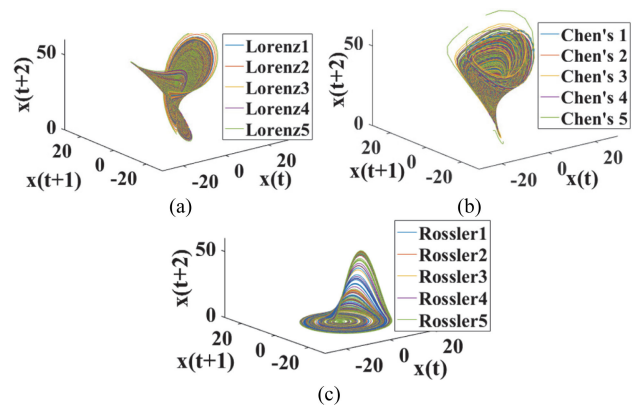

Fig. 3. 3-D reconstructed attractors of (a) Lorenz, (b) Chen, and (c) Rössler's system.

Five groups of attractors with different initial values are plotted in three dimensions, as shown in Fig. 3(a), (b), and (c), respectively. We can see that the shapes of Lorenz, Rössler, and Chen's attractors are quite different. For each kind of system, even if the initial value is different, after a period of evolution, the shapes of attractors are quite similar.

To further quantify the shape characteristics of the chaotic attractor, we use four shape feature functions, D2, A1, T1, and T2 (we will define the above-mentioned four functions in Section III). Then, histogram statistics are performed on the four morphological features. Now, we obtain their corresponding probability distribution plots, defined as the MD. We compute four MDs of Lorenz, Rössler, and Chen's attractors with five different initial values respectively and plot them in Fig. 4. As illustrated, attractors of different chaotic systems have very different morphological characteristics.

C. Chaotic Characteristics of the Intensity Sequence of the Flame Video in a Rotary Kiln

The flickering frequency of the flame is a criterion for combustion stability recognition [8], but it cannot be accurately calculated from the video due to the blur caused by smoke and dust in the industrial environment. To extract features more rapidly and robustly from blurred images, we calculate average intensity of whole image in flame video and form intensity sequence to study its dynamic characteristics. Although the change of image intensity cannot completely equal to the flicker frequency of

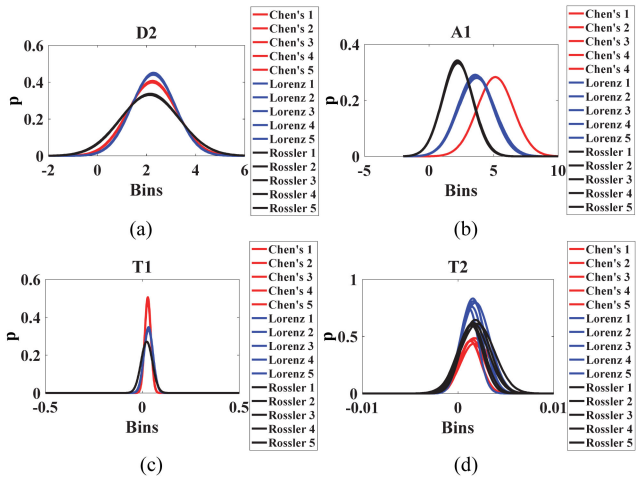

Fig. 4. Morphology distribution (MD) of (a) D2, (b) A1, (c) T1, and (d) T2 extracted from Chen, Lorenz, and Rössler's attractors with five sets of different initials separately.

the flame, from the perspective of the long-term change trend, the change of the image intensity can represent the flickering frequency of the flame to a certain extent. In fact, it is one of the effective approaches for the workers at the industrial site to judge combustion condition by observing the intensity change of the flame image based on their experience.

To reasonably analyze the internal dynamics of the intensity sequence, we calculate the maximum Lyapunov exponent (MLE) and the fractal dimension (FD) of the intensity series to analyze whether chaotic characteristics exist and what the degree of chaos is. The MLE represents the numerical characteristics of the average exponential divergence of the attractor trajectory in the phase space [32]. If the MLE is greater than zero, the system is chaotic. In addition, the fine structure of trajectories with self-similarity is called fractal. FD spectrum (FDS) reflects the effectiveness of the space occupied by the complex attractor. It is a measure of the irregularity of attractors. The degree of chaos in the system can be described by FDS. The span of the FDS reflects the irregularity and unevenness of the system. The larger the span of the FDS is the greater the degree of chaos.

We randomly selected six flame videos covering two combustion conditions and extracted six intensity sequences. The Wolf algorithm is introduced to estimate the MLE for the raw signal and signals after being filtered by wavelet, Gabor, moving smooth and Savitzky Golay filters. The MLEs of six intensity sequences are shown in Fig. 5(a), and they are always greater than zero with or without denoising. The FDS is estimated by the wavelet p-leader method [33]. As illustrated in Fig. 5(b), the FDS is a unimodal function, where h is the Hurst exponent, and D(h) is the multifractal spectrum. The greater the span of the FDS is, the greater the irregularity and unevenness, and the stronger the chaotic characteristics. Therefore, we believe that the intensity signal extracted from a flame video has chaotic characteristics regardless of the presence of noise. Moreover, Fig. 5(b) show the difference in the spans of the FDSs of the intensity signal

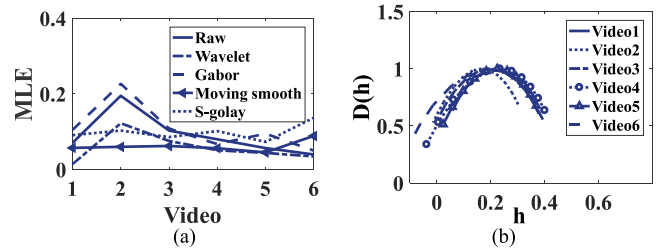

Fig. 5. MLEs and the FDS of six intensity signals. (a) MLEs. (b) FDS.

extracted under the stable and unstable combustion conditions is small. These FDSs are basically left-biased, and the distribution range is basically the same. Therefore, these general methods of judging the chaos are not suitable for distinguishing whether flame combustion is stable.

III. Dynamic Feature Extraction Based on a Chaotic Attractor

According to Figs. 3 and 4, the two chaotic systems have distinct morphology and evolution attractor characteristics. Thus, when the operation rules of the system are different, the morphology of the corresponding attractors is distinct. When the combustion condition of the furnace changes, the operation rules of the system changes. This situation will lead to the distortion of the chaotic attractor.

Based on this result, we propose recognizing the combustion condition based on chaotic characteristics analysis. First, we reconstruct the chaotic attractors from the intensity sequence. MI measures the interdependence between $x_n(i)$ and $x_n(i+\tau)$ both of length n intercepted from data $x(t)$. The first local minimum of the autocorrelation curve is selected as τ. FNN extends the 1-D data to the high-dimensional data and observes the number of neighbors of a certain point. When the number of neighbors does not decrease, the expansion stops. The corresponding dimension is the minimum embedded dimension m. The chaotic attractors can be reconstructed as X_i. If the dimension of the reconstructed attractor is more than three, the chaotic attractor cannot be visualized directly. To quantify the morphology and evolution characteristics of chaotic attractors, we extract the TEFs and MDFs of attractors reconstructed from intensity sequences. The TEF describes the changes in dynamic systems over time, and the MDF describes the shape of attractors in high-dimensional space.

A. TEF

The evolutionary nature of one system trajectory can be visualized by the RP, which is an important method for analyzing the periodicity, chaos, and nonstationarity of a time-series. The RP is a time-series data processing method that can build a 2-D matrix from 1-D data $\boldsymbol{x}_i$ to demonstrate self-correlation between data. To make the plot, take X_i as the location of the trajectory at time i and count as a recurrence any time X_j gets sufficiently close (within ε) to X_i. The recurrence matrix is as follows:

$$\mathbf{R}_{i,j}$$

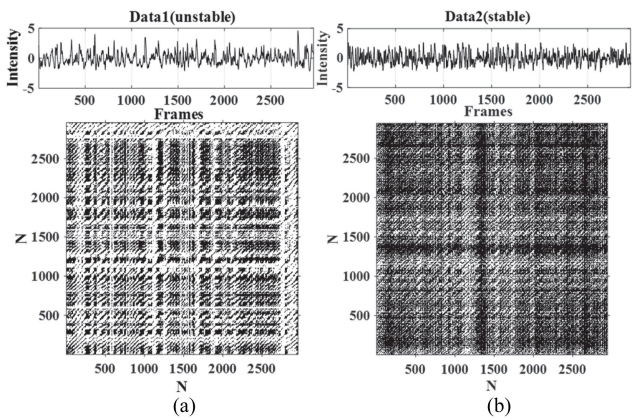

Fig. 6. RPs of (a) Data1 (unstable) and (b) Data2 (stable).

$$= \Theta(\varepsilon - ||\mathrm{X}_i - \mathrm{X}_j||), i, j = 1, 2, 3, \ldots, N = n - (m-1)\tau \tag{5}$$

where X_i and X_j are two different state points on the phase space trajectory representing the states at times i and j, respectively, n is the number of $x(t)$, N is the number of reconstructed phase points of attractors, and Θ is the Heaviside step function.

The appearance of line segments in the RP indicates that the system contains a deterministic characteristic. The number, length, and distribution of line segments in the RP reflect the characteristics of the system from different aspects. There are three typical small-scale structures (textures) in the RP, containing single dots, diagonal lines, and vertical/horizontal lines:

1) a single dot means that this state is rare and short-lived, or the system fluctuates strongly;
2) a diagonal line of length l illustrates that one segment of the phase space trajectory parallels another approximately for time l. The diagonal structure in the RP can reflect the determinism and periodicity of the system;
3) a vertical/horizontal line of size v expresses that the system does not change or changes very slowly for time v.

RPs of Data1 and Data2 are built as shown in Fig. 6. In Fig. 6(b), the pattern distribution is more regular, the diagonal lines are clearer and signs of almost periodic trajectories are apparent. The internal regularity of the intensity sequence extracted from the flame video is relatively strong when the combustion is stable. This result shows that compared with unstable combustion, flame flickering during stable combustion has a certain regularity. When the combustion condition changes, the flickering rate of the coal-fired flame becomes more chaotic, and the diagonal structure in the RP of Data1 is almost destroyed.

We extracted five TEFs from the RP formed by the flame videos to reflect the dynamic changes of the furnace system.

1) Determinism (DET):

$$DET = \frac{\sum_{l=l_{\min}}^{N} lP(l)}{\sum_{l}^{N} lP(l)} \tag{6}$$

where $l_{\min}$ is considered the shortest diagonal length, reflecting the determinism of the system, and $P(l)$ is the number of diagonal lines of length l. The formula for $P(l)$ is given as follows:

$$P(l) = \sum_{i,j=1}^{N} (1 - \mathbf{R}_{i-1,j-1})(1 - \mathbf{R}_{i+l,j+l}) \prod_{k=0}^{l-1} \mathbf{R}_{i+k,j+k}. \tag{7}$$

The threshold $l_{\min}$ discards the diagonal lines that are formed by the tangential motion of the phase space trajectory. *DET* is the ratio of the recurrence points forming diagonal lines to all recurrence points.

2) Average Diagonal Line Length (L):

$$L = \frac{\sum_{l=l_{\min}}^{N} lP(l)}{\sum_{l=l_{\min}}^{N} P(l)} \tag{8}$$

where L represents the average time between two parallel segments running closely in the phase space trajectory. It is the ratio of all the recurrence points forming diagonal lines to the total number of diagonal lines whose lengths are greater than $l_{\min}$.

3) Entropy (ENTR):

$$ENTR = -\sum_{l=l_{\min}}^{N} p(l) \ln p(l) \tag{9}$$

where $p(l) = P(l)/N_l$ is the probability of finding a diagonal line of length l in the RP. *ENTR* reflects the complexity of the diagonal line length in the RP instead of the complexity of datasets.

4) Laminarity (LAM):

$$LAM = \frac{\sum_{v=v_{\min}}^{N} vP(v)}{\sum_{v=1}^{N} vP(v)} \tag{10}$$

where $v_{\min}$ denotes the minimum length describing the laminarity of the system. $P(v)$ represents the number of vertical/horizontal lines of length v in the RP, and its definition is given as follows:

$$P(v) = \sum_{i,j=1}^{N} (1 - \mathbf{R}_{i,j})(1 - \mathbf{R}_{i,j+v}) \prod_{k=0}^{v-1} \mathbf{R}_{i,j+k}. \tag{11}$$

Similar to *DET*, the ratio of the recurrence points forming the vertical line structure to all recurrence points was recorded as *LAM*. Laminarity means that the state of the system does not change over time or that the state changes very slowly.

5) Trapping Time (TT):

$$TT = \frac{\sum_{v=v_{\min}}^{N} vP(v)}{\sum_{v=v_{\min}}^{N} P(v)} \tag{12}$$

which estimates the average time that the system maintains a specific state. Therefore, the longer the system maintains a certain state, the greater the value of *TT* is.

From Data1 and Data2 with a length of 15 000, we intercept the data with a sliding window. The window length is 3000, and the step size is 160. The intercepted data, subsequences $\mathrm{Data1_s}$ and $\mathrm{Data2_s}$, are obtained. Then, PSR is performed on each $\mathrm{Data1_s}$ and $\mathrm{Data2_s}$. Finally, 75 sets of TEFs extracted from the reconstructed $\mathrm{Data1_s}$ and $\mathrm{Data2_s}$ are shown in Fig. 7. The blue line represents the stable condition, and the red line represents the unstable condition. The horizontal axis in the figure is the

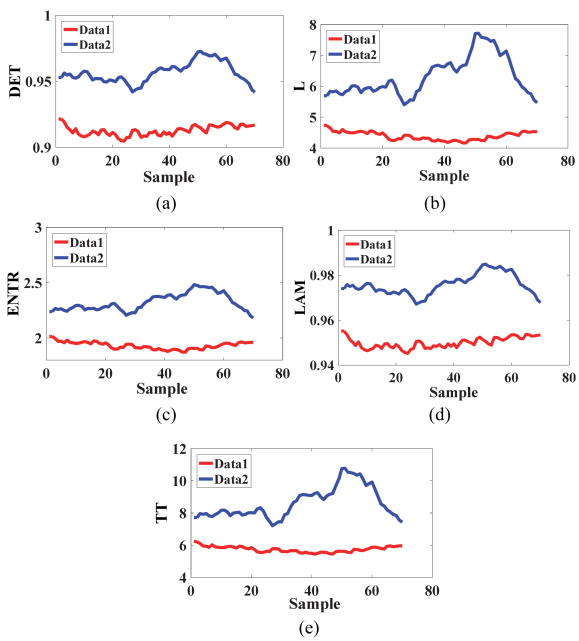

Fig. 7. TEFs of Data1 (unstable) and Data2 (stable).

number of times that TEFs are extracted, and the vertical axis is the value of each feature. The blue line represents the stable condition, and the red line represents the unstable condition. We can see that the features of Data2 are larger than those of Data1. When the combustion condition is stable, the flame in the furnace flickers more regularly. This behavior will cause a longer diagonal structure in the RP. Thus, TEFs should be smaller when the combustion of the furnace fluctuates more.

B. MDF

The shape of the chaotic attractor in the high-dimensional phase space characterizes the operation rules of the dynamic system. Thus, we use the MD to represent the shape of chaotic attractors. We adopt four shape feature functions, D2, A1, T1, and T2, to measure the relationship between high-dimensional phase points. Some studies have shown that the MD can be used as a feature representation of any n-dimensional phase space [34].

1) D2 :

$$D2 = ||\mathrm{X}_i - \mathrm{X}_j||_2 \tag{13}$$

represents the distance between two random space points.

2) A1:

$$A1 = \arccos(\mathbf{a} \cdot \mathbf{b} / |\mathbf{a}|\,|\mathbf{b}|) \tag{14}$$

represents the angle formed between any three-space points.

3) T1:

$$T1 = \sqrt{|\mathbf{a}|^2|\mathbf{b}|^2 - (\mathbf{a} \cdot \mathbf{b})^2} \tag{15}$$

represents the square root of the area of the triangle formed by three random space points. **a** and **b** are the vectors calculated from the two random phase points.

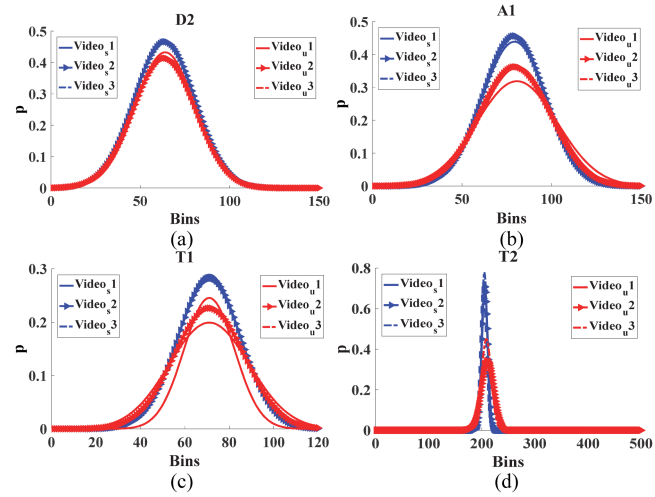

Fig. 8. MD of (a) D2, (b) A1, (c) T1, and (d) T2, the subscript s represents stable data, and u represents unstable data.

4) T2:

$$T2 = \frac{1}{6}\mathbf{abc}\sqrt{\begin{vmatrix} 1 & \cos\alpha & \cos\beta \\ \cos\alpha & 1 & \cos\gamma \\ \cos\beta & \cos\gamma & 1 \end{vmatrix}} \tag{16}$$

represents the volume of a tetrahedron formed by any four-phase points. **a**, **b** and **c** are the vectors calculated from the two random phase points. α, β, and γ are the angles formed between **a**, **b** and **c**.

We calculated the MDs of three stable sequences and three unstable sequences. The distributions are shown in Fig. 8. To quantify the distance between MDs, the extreme value (ep), kurtosis (k), and skewness (s) of distributions are extracted as MDFs. s is a measure of the asymmetry of a probability distribution. k is a measure of the tailedness of a probability distribution. It is generally used to identify outliers in the given data.

Similar to extracting TEFs, we extracted 75 sets of MDFs plotted in Fig. 9. The blue line represents Data2 (stable condition), and the red line represents Data1 (unstable condition). We find that ep, k, and s of D2, T1, and T2 of Data2 are higher than those of Data1. In addition, the ep, k, and s of A1 of Data2 are lower than those of Data1. This is because the phase point distribution of the attractor in the stable combustion condition is relatively concentrated, and the trajectory change has a certain periodicity, while the phase point distribution of the attractor phase point in the unstable combustion condition is more dispersed, and the phase point trajectory changes more chaotically.

IV. Experiments

In this section, the experiments on industrial data were carried out in the MATLAB R2016b programming language with a 3.60-GHz Intel(R) Core (TM)2 i7–7700 CPU computer and 8.0 GB of memory under Microsoft Windows 10.

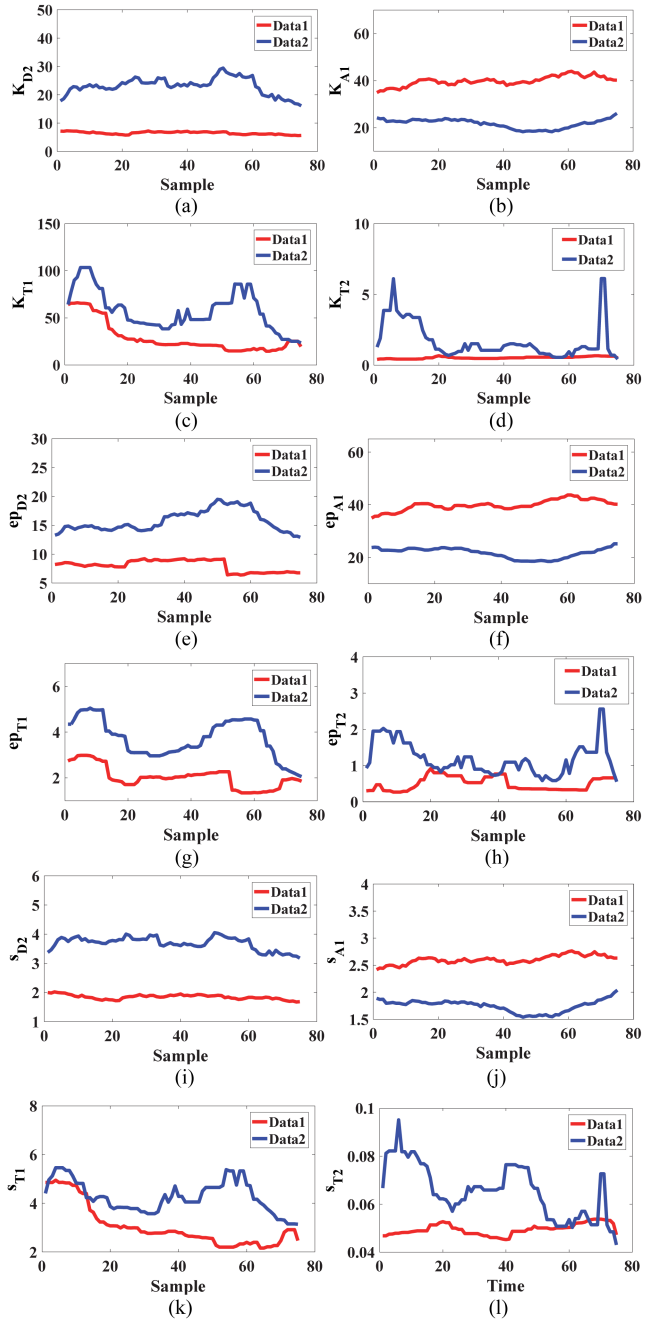

Fig. 9. Twelve MDFs of Data1 and Data2, where *ep* is extreme points, *k* is kurtosis, and *s* is skewness.

A. Description of Industry Data

In total, 17 sets of 10-min videos are taken by a color charge-coupled device (CCD) camera installed in the peephole of the discharge port of the kiln. The camera we used was an HCC series high-temperature camera, and its model was HCC-8655PT. The output of the CCD after digitization by an image grabber card turns into the digital image. The conversion frequency of the frame grabber is 25 frames per second(fps). According to the researches of Lu [35], Hamins [36], and Gotoda [37], the flicker frequency of coal-fired flame is about 10 Hz. Therefore, sampling rate of 25 fps is greater than twice of frequency of the flame flicker, which can ensure the integrity and accuracy of the signal sampling. To analyze the combustion condition of the coal-fired furnace, we used the same camera to shoot flame videos over a long period in the #1 rotary kiln of Zhong Zhou Aluminium Corporation in China. These videos cover stable and unstable combustion conditions.

We extract each frame of the image from the video and calculate its average grey value I to form the intensity sequence. The equation is as follows:

$$I = \frac{\sum_{k=1}^{row} \sum_{p=1}^{col} grayscale_{k,p}}{row \times col}. \tag{17}$$

In our experiment, $row = 704$ and $col = 576$ are the dimensions of the flame image. Then, an intensity sequence of length 15 000 is extracted from each video. Finally, seventeen sets of intensity sequences are used to extract the dynamic features of the combustion condition.

TABLE I
OPTIMIZING PARAMETERS

	Length	*DET*	*L*	*ENTR*	*LAM*	*TT*
Unstable combustion	500	0.9058	3.6470	1.5296	0.8781	4.8444
	1000	0.9043	3.9360	1.8488	0.9362	5.4036
	3000	0.9289	4.8105	2.0363	0.9568	6.8722
	5000	0.9043	3.8377	1.6469	0.9061	5.0890
Stable combustion	500	0.9168	4.9172	2.0364	0.9516	6.1279
	1000	0.9333	5.0950	2.1128	0.9598	7.2256
	3000	0.9538	5.9950	2.6099	0.9788	8.1867
	5000	0.9481	4.5585	2.2344	0.9352	6.3047

B. Selection of the Data Length

To find the appropriate data length to extract TEFs and MDFs with higher separability, we carried out combustion condition analysis on data of different lengths. Use the first subsequence intercepted in Data1(unstable) and Data2(stable), and select the subsequence length of the comparison test as 500, 1000, 3000, 5000, and 7000, respectively.

To the best of authors' knowledge, L in the RP with a high value and uniform distribution can better present the characteristics of one system. We compared the obtained L value with data of different lengths. The comparison results are in Table I. Through experimental results, we found that when the data length n is 3000, the separability of TEFs is higher and the L in TEFs is higher. The distinguishability of the TEFs has been visualized in Fig. 7 when n is 3000.

In addition, the experimental results of the relationship between the MD and the data length are shown in Fig. 10. Different linear representations of MDs are calculated under different data lengths. It can be concluded that the MDFs are not very sensitive to changes in data length. Fig. 9 also shows the distinguishability of MDFs when the data length is 3000. After comprehensive consideration, in the process of combustion condition analysis, n will be set to 3000.

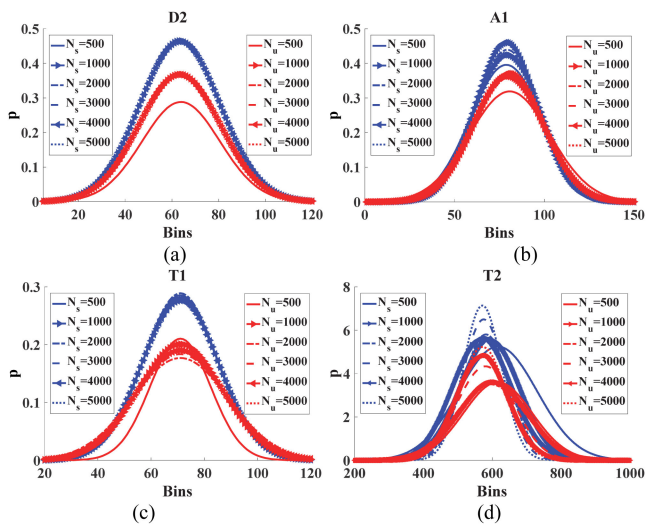

Fig. 10. MD of (a) D2, (b) A1, (c) T1, and (d) T2 calculated with different data lengths from 500 to 5000, where N represents the data length.

C. Combustion Condition Identification

First, we acquire1 50 000 × 17 sets of intensity sequences from 17 sets of flame videos. Then feature information of the intensity sequence is extracted through the sliding window, the window length is 3000, and the step size is 160. Extract a set of feature TEFs and MDFs we proposed from one window data, and finally, we obtain 2057 sets of feature samples from 17 sets of intensity sequences

Then we need to get the labels of the extracted features. Several experienced kiln workers watched seventeen sets of flame videos and judged the condition of each set of videos based on their experience. The kiln worker helped us mark the specific time when the combustion condition changes. The feature extracted from the stable combustion period is marked as label 1, and the feature extracted from the unstable combustion period is marked as label 0. When the conversion time the workers marked is included in the subsequence, the feature extracted from the subsequence is marked as 0. Finally, 2057 samples are obtained from 17 flame videos. Among them, 893 are unstable samples, and 1164 are stable samples. In total, 80% of the samples are used for training the classifier, and 20% are used for testing.

A decision tree classifier is employed to recognize the combustion condition. The final classifier is developed using the complete training set. It is retrained with the optimal parameters by all the training datasets and is used to classify the combustion condition on the testing set. The average classification accuracy obtained for 50 trials is given in Table I, which shows that both classifiers achieve a recognition accuracy of more than 90%. The results demonstrate the effectiveness of the condition recognition method proposed in this article.

Table II shows that when single-frame images or multiframe images cannot extract flame features in the video, the recognition results of the methods in references [6] and [15] are not very satisfactory. Even if the method in reference [15] considers fusing the features of multiple frames of images within one second, the blurry images that suddenly appear during the stable combustion process will still affect the recognition results. However, the method proposed in this article avoids having to obtain achievable information from the image. When single-frame images or multiple-frame images cannot extract flame features, the intensities of fuzzy images have little effect on combustion analysis compared to the overall intensity sequence. Especially when the flame continues to deflagrate and other extreme situations occur, the quality of consecutive multiple frames of images is extremely poor. At this time, the proposed method takes the change of the intensity sequence as a dynamic feature. Therefore, our method obtains higher recognition accuracy and stronger robustness and is more suitable for combustion condition analysis in the context of coal-burning industries.

TABLE II
RECOGNITION ACCURACY

	Training	Testing
TEFs	96.6%	93.9%
MDFs	94.8%	92.6%
All features	97.8%	95.9%
Comparative features[6]	92.7%	90.4%
Comparative features[15]	78.1%	71.2%

TABLE III
EXPERIMENTAL RESULTS OF ROBUSTNESS TEST

		Training	Testing
Intensity with Gaussian white noise and outlies	TEFs	95.2%	93.6%
	MDFs	94.5%	92.1%
	All features	97.0%	94.8%

D. Robustness Test

To verify the robustness of the proposed method, we added Gaussian white noise with a signal-to-noise ratio of 1 dB to the raw intensity sequence, and randomly replaced 1000 light intensity points with outliers for recognition of combustion condition. The recognition results are shown in Table III. Table III shows that the method and the two features proposed in this article are less affected by noise and outliers and have strong robustness.

V. CONCLUSION

The main content of this article was that we proposed an approach based on chaos dynamic system analysis for industrial flame video combustion condition recognition. This method has high recognition accuracy and strong robustness. And we find for the first time that there were chaotic characteristics in the intensity sequence of industrial flame video. When the combustion conditions were different, the chaotic characteristics of the intensity sequence were significantly different. Based on this, we first analyzed the stability of the lighting sequence extracted

from the flame video from the perspective of a dynamic system, and designed a set of TEFs and MDFs to quantify the trajectory and morphological characteristics of the chaotic attractor in the high-dimensional phase space.

The proposed method was supported by two theories. First, compared with unstable combustion, the flame of stable combustion has more regular flicker and movement to a certain extent. On this basis, the RP was introduced to extract the evolution characteristics of the intensity sequence. The texture in the RP can reflect the period of the dynamic system. Therefore, TEFs were suitable for describing the flickering rate of the flame intensity sequence. Second, when the combustion condition of the furnace changes, the operation rules were also changed. Therefore, the chaotic attractors have been distorted. Extracting the morphology features of the chaotic attractor helps characterize the combustion condition. The features we proposed were more robust, even if the video was blurred.

In the future, we will further improve the real-time performance and accuracy of the algorithm while exploring other possibilities of combining these features with on-site thermal data to better identify combustion conditions.

References

[1] B. Mohan and S. Mariappan, "Nonlinear stability analysis of intrinsic thermoacoustic modes in a one-dimensional longitudinal combustor," *Combustion Flame*, vol. 215, pp. 309–323, 2020.

[2] M. A. A. Mendes, J. M. C. Pereira, and J. C. F. Pereira, "A numerical study of the stability of one-dimensional laminar premixed flames in inert porous media," *Combustion Flame*, vol. 153, no. 4, pp. 525–539, 2008.

[3] R. Sui and J. Mantzaras, "Combustion stability and hetero-/homogeneous chemistry interactions for fuel-lean hydrogen/air mixtures in platinum-coated microchannels," *Combustion Flame*, vol. 173, pp. 370–386, 2016.

[4] K. Muhammad, J. Ahmad, and S. W. Baik, "Early fire detection using convolutional neural networks during surveillance for effective disaster management," *Neurocomputing*, vol. 288, pp. 30–42, 2018.

[5] Y. Han, C. Zhang, L. Wang, and Y. Zhang, "Industrial IoT for intelligent steelmaking with converter mouth flame spectrum information processed by deep learning," *IEEE Trans. Ind. Informat.*, vol. 16, no. 4, pp. 2640–2650, Apr. 2020.

[6] H. Chen, X. Zhang, P. Hong, H. Hu, and X. Yin, "Recognition of the temperature condition of a rotary kiln using dynamic features of a series of blurry flame images," *IEEE Trans. Ind. Informat.*, vol. 12, no. 1, pp. 148–157, Feb. 2016.

[7] W. Li, D. Wang, and T. Chai, "Flame image-based burning state recognition for sintering process of rotary kiln using heterogeneous features and fuzzy integral," *IEEE Trans. Ind. Informat.*, vol. 8, no. 4, pp. 780–790, Nov. 2012.

[8] M. G. De Giorgi, A. Sciolti, S. Campilongo, and A. Ficarella, "Image processing for the characterization of flame stability in a non-premixed liquid fuel burner near lean blowout," *Aerosp. Sci. Technol.*, vol. 49, pp. 41–51, 2016.

[9] Z. Wang, K. Pan, D. Cai, B. Jin, and P. Liu, "Experimental study of aluminum combustion in solid propellant by using photomicrography and digital in-line holography," in *Proc. 11th Int. Conf. Mech. Aerosp. Eng.*, 2020, pp. 168–172.

[10] B. Hyeon, K. Sungshin, W. Bo-Hyeun, L. M. Hyung, and F. Harashima, "Flame detection for the steam boiler using neural networks and image information in the Ulsan steam power generation plant," *IEEE Trans. Ind. Electron.*, vol. 53, no. 1, pp. 338–348, Feb. 2006.

[11] P. Tóth, A. Garami, and B. Csordás, "Image-based deep neural network prediction of the heat output of a step-grate biomass boiler," *Appl. Energy*, vol. 200, pp. 155–169, 2017.

[12] O. Choi, J. Choi, N. Kim, and M. Lee, "Combustion instability monitoring through deep-learning-based classification of sequential high-speed flame images," *Electronics*, vol. 9, 2020, Art. no. 848.

[13] M. Najarnikoo, M. Z. Targhi, and H. Pasdarshahri, "Experimental study on the flame stability and color characterization of cylindrical premixed perforated burner of condensing boiler by image processing method," *Energy*, vol. 189, 2019, Art. no. 116130.

[14] C. Jeong, J. Bae, T. Kim, J. Yoon, S. Joo, and Y. Yoon, "Investigation of flashback characteristics coupled with combustion instability in turbulent premixed bluff body flames using high-speed OH-PLIF and PIV," in *Proc. Combustion Inst.*, vol. 36, no. 2, pp. 1861–1868, 2017.

[15] J. Matthes, P. Waibel, M. Vogelbacher, H. J. Gehrmann, and H. B. Keller, "A new camera-based method for measuring the flame stability of non-oscillating and oscillating combustions," *Exp. Thermal Fluid Sci.*, vol. 105, pp. 27–34, 2019.

[16] D. Sun, G. Lu, H. Zhou, Y. Yan, and S. Liu, "Quantitative assessment of flame stability through image processing and spectral analysis," *IEEE Trans. Instrum. Meas.*, vol. 64, no. 12, pp. 3323–3333, Dec. 2015.

[17] İ. Yilmaz, B. Alabaş, M. Taştan, and G. Tunç, "Effect of oxygen enrichment on the flame stability and emissions during biogas combustion: An experimental study," *Fuel*, vol. 280, 2020, Art. no. 118703.

[18] Z. Han, M. M. Hossain, Y. Wang, J. Li, and C. Xu, "Combustion stability monitoring through flame imaging and stacked sparse autoencoder based deep neural network," *Appl. Energy*, vol. 259, 2020, Art. no. 114159.

[19] Z. Wang, C. Song, and T. Chen, "Deep learning based monitoring of furnace combustion state and measurement of heat release rate," *Energy*, vol. 131, pp. 106–112, 2017.

[20] H. Chen, T. Yan, and X. Zhang, "Burning condition recognition of rotary kiln based on spatiotemporal features of flame video," *Energy*, vol. 211, 2020, Art. no. 118656.

[21] W. Du, M. Kang, and M. Pecht, "Fault diagnosis using adaptive multifractal detrended fluctuation analysis," *IEEE Trans. Ind. Electron.*, vol. 67, no. 3, pp. 2272–2282, Mar. 2020.

[22] S. Das, A. K. Pradhan, A. Kedia, S. Dalai, B. Chatterjee, and S. Chakravorti, "Diagnosis of power quality events based on detrended fluctuation analysis," *IEEE Trans. Ind. Electron.*, vol. 65, no. 9, pp. 7322–7331, Sep. 2018.

[23] X. Zhang, L. Zhang, H. Chen, and B. Dai, "Prediction of coal feeding during sintering in a rotary kiln based on statistical learning in the phase space," *ISA Trans.*, vol. 83, pp. 248–260, 2018.

[24] M. Lv, X. Zhang, H. Chen, Y. Zhou, and J. Li, "Chaotic and multifractal characteristic analysis of noise of thermal variables from rotary kiln," *Nonlinear Dyn.*, vol. 99, no. 4, pp. 3089–3111, 2020.

[25] F. Takens, "Detecting strange attractors in turbulence," in *Dynamical Systems and Turbulence, Warwick 1980*. Berlin, Germany: Springer, 1981, pp. 366–381.

[26] A. M. Fraser and H. L. Swinney, "Independent coordinates for strange attractors from mutual information," *Phys. Rev. A*, vol. 33, no. 2, pp. 1134–1140, 1986.

[27] M. B. Kennel, R. Brown, and H. D. I. Abarbanel, "Determining embedding dimension for phase-space reconstruction using a geometrical construction," *Phys. Rev. A*, vol. 45, no. 6, pp. 3403–3411, 1992.

[28] N. Marwan, M. C. Romano, M. Thiel, and J. Kurths, "Recurrence plots for the analysis of complex systems," *Phys. Rep.*, vol. 438, no. 5, pp. 237–329, 2007.

[29] E. N. Lorenz, "Deterministic nonperiodic flow," *J. Atmos. Sci.*, vol. 20, no. 2, pp. 130–141, Mar. 1963.

[30] J. C. Sprott and L. I. Chunbiao, "Asymmetric bistability in the Rössler system," *Acta Physica Polonica B*, vol. 48, no. 1, pp. 97–107, 2017.

[31] T. Zhou, Y. U. N. Tang, and G. Chen, "Chen's attractor exists," *Int. J. Bifurcation Chaos*, vol. 14, no. 9, pp. 3167–3177, 2004.

[32] J. P. Eckmann and D. Ruelle, "Ergodic theory of chaos and strange attractors," *Rev. Modern Phys.*, vol. 57, no. 3, pp. 617–656, 1985.

[33] S. Jaffard *et al.*, "P-Exponent and p-leaders, Part I: Negative pointwise regularity," *Physica A, Stat. Mechanics Appl.*, vol. 448, pp. 300–318, 2016.

[34] R. Osada, T. Funkhouser, B. Chazelle, and D. Dobkin, "Shape distributions," *ACM Trans. Graph.*, vol. 21, pp. 807–832, 2002.

[35] G. Lu, Y. Yan, M. Colechin, and R. Hill, "Monitoring of oscillatory characteristics of pulverized coal flames through image processing and spectral analysis," *IEEE Trans. Instrum. Meas.*, vol. 55, no. 1, pp. 226–231, Feb. 2006.

[36] A. Hamins, J. C. Yang, and T. Kashiwagi, "An experimental investigation of the pulsation frequency of flames," *Symp. (Int.) Combustion*, vol. 24, no. 1, pp. 1695–1702, 1992.

[37] H. Gotoda, T. Ueda, I. G. Shepherd, and R. K. Cheng, "Flame flickering frequency on a rotating Bunsen burner," *Chem. Eng. Sci.*, vol. 62, no. 6, pp. 1753–1759, 2007.

Yu Jiang received the B.S. degree in automation in 2017 from Control Science and Engineering, Hunan University, Changsha, China, where she is currently working toward the Ph.D. degree in control theory and control science.

Her research interests include nonlinear analysis, chaos theory, pattern recognition, and machine learning for industrial process applications.

Hua Chen received the B.S., M.S., and Ph.D. degrees in control science and engineering from Hunan University, Changsha, China, in 1996, 2002, and 2014, respectively.

She is currently an Associate Professor with the College of Computer Science and Electronic Engineering, Hunan University. Her research interests include image and video processing, machine learning, and computer vision.

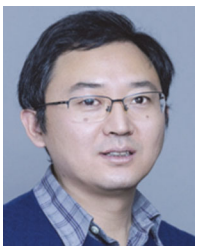

Xiaogang Zhang (Member, IEEE) received the bachelor's, master's, and Ph.D. degrees in control theory and engineering from Hunan University, Changsha, China, in 1996, 1999, and 2003, respectively.

From 2015 to 2016, he was a Visiting Scholar with the Department of Computer Science, Brandeis University, Boston, MA, USA. He has been a Full Professor with the College of Electrical and Information Engineering, Hunan University. He has applied his expertise extensively in industrial practice, particularly in metallurgical process control and industrial robots. His research interests include pattern recognition and data mining for industrial control systems.

Yicong Zhou (Senior Member, IEEE) received the B.S. degree from Hunan University, Changsha, China, in 1992, and the M.S. and Ph.D. degrees from Tufts University, Massachusetts, MA, USA, in 2008 and 2010 respectively, all in electrical engineering.

He is currently a Professor with the Department of Computer and Information Science, University of Macau, Macau, China. His research interests include image processing, computer vision, machine learning, and multimedia security.

Dr. Zhou is a Fellow of SPIE (the Society of Photo-Optical Instrumentation Engineers) and was recognized as one of the "World's Top 2% Scientists" and one of the "Highly Cited Researchers" in 2020. He received the Third Price of Macao Natural Science Award as a sole winner in 2020 and a corecipient in 2014. Since 2015, he has been a leading Co-Chair of Technical Committee on Cognitive Computing with the IEEE Systems, Man, and Cybernetics Society. He serves as an Associate Editor for the IEEE Transactions on Neutral Networks and Learning Systems, IEEE Transactions on Circuits and Systems for Video Technology, IEEE Transactions on Geoscience and Remote Sensing, and four other journals.

Lianhong Wang received the B.S. degree in circuit and system major, the M.S. degree in control theory, and the Ph.D. degree in control engineering from Hunan University, Changsha, China, in 1993, 2002, and 2009, respectively.

From 2011 to 2012, she was a Visiting Scholar with Brandeis University, Boston, MA, USA. She is currently an Associate Professor with the College of Electrical and Information Engineering, Hunan University. Her research interests include signal/image processing, data mining, and modern network communication technology.